

See discussions, stats, and author profiles for this publication at: <https://www.researchgate.net/publication/10988172>

Time-Resolved Dissociation of the Light-Harvesting 1 Complex of *Rhodospirillum rubrum*, Studied by Infrared Laser Temperature Jump †

ARTICLE in *BIOCHEMISTRY* · JANUARY 2003

Impact Factor: 3.02 · DOI: 10.1021/bi0269005 · Source: PubMed

CITATIONS

11

READS

20

5 AUTHORS, INCLUDING:



Anjali Pandit

Leiden University

28 PUBLICATIONS 273 CITATIONS

SEE PROFILE



Ivo H M Van Stokkum

VU University Amsterdam

280 PUBLICATIONS 10,114 CITATIONS

SEE PROFILE



Rienk van Grondelle

VU University Amsterdam

647 PUBLICATIONS 23,660 CITATIONS

SEE PROFILE

Time-Resolved Dissociation of the Light-Harvesting 1 Complex of *Rhodospirillum rubrum*, Studied by Infrared Laser Temperature Jump[†]

Anjali Pandit,^{*,‡} Hairong Ma,[§] Ivo H. M. van Stokkum,^{||} Martin Gruebele,^{§,⊥} and Rienk van Grondelle^{||}

Department of Structural Biology and Faculty of Earth and Life Sciences and Division of Physics and Astronomy, Faculty of Sciences, Vrije Universiteit Amsterdam, De Boelelaan 1087, 1081 HV Amsterdam, The Netherlands, and Departments of Chemistry and Physics and Center for Biophysics and Computational Biology, University of Illinois at Urbana-Champaign, Urbana, Illinois 61801

Received September 25, 2002; Revised Manuscript Received November 18, 2002

ABSTRACT: For the first time, data are presented on the time-resolved disassembly reaction of a highly organized membrane protein complex in vitro. The photosynthetic core light-harvesting complex of the bacterial strain *Rhodospirillum rubrum* G9 consists of 12–16 dimeric subunits that in vivo are associated with the photosynthetic reaction center in a ringlike manner. Isolated in a detergent solution, its appearance either as a ringlike complex (called B873 and absorbing at 873 nm), subunit dimer (called B820 and absorbing at 820 nm), or monomeric form (called B777 and absorbing at 777 nm) is strongly temperature-dependent. In thermodynamic equilibria between B820 and B873, intermediate-sized complexes have also been observed that have absorption maxima around 850 nm. It is unknown whether these structures appear as intermediates in the kinetic B820–B873 (dis)assembly reaction. In this paper disassembly of the light-harvesting complex into its dimeric subunits was followed spectroscopically on a time scale up to 200 ms, upon applying an infrared laser-induced temperature jump. The full dissociation process appears to take place on a time scale of tens to hundreds of milliseconds, the rates becoming faster at higher starting temperatures. Applying the same technique, the dissociation reaction of dimeric subunits into monomers also could be established. This dissociation process occurred on a much faster time scale and took place within the 500 μ s response time of our detection system.

Transmembrane proteins are generally complexes consisting of arranged α -helical bundles that span the lipid bilayer. Their specific functioning highly depends on correct folding of the separate transmembrane segments and the precise pattern of their assembly via helix-helix interaction; however, very little is known about the process of their (dis)assembly. Examples are the light-harvesting complexes in photosynthesis that are responsible for the capture of light and energy transfer to the reaction center. These complexes consist of pigment-binding polypeptides embedded in the photosynthetic membrane. Due to the specific assembly of the polypeptides, their pigment arrangement is optimized for trapping of light using excitonic interactions and energy

transfer between the pigments. In purple non-sulfur bacteria, two light-harvesting complexes exist: the peripheral antenna (LH2)¹ and the core antenna (LH1) which surrounds the reaction center (RC) where charge separation takes place (1, 2). Both types of complexes appear to consist of ringlike structures of heterodimeric protein–pigment subunits. For LH2 the structure has been resolved to high resolution for *Rhodopseudomonas acidophila* (3) and for *Rhodospirillum rubrum* (4) and consists of a ring of nine and eight pigment–protein subunits, respectively. For LH1 only a low-resolution structure for the strain *Rs. rubrum* exists (5). Knowledge of the low-resolution of LH1 combined with the high-resolution of LH2 has stimulated detailed modeling (6). According to these models, the LH1 consists of a ring of 16 pigment–protein subunits, that encircles the RC. The LH1 and LH2 subunits consist of pigment-binding heterodimers of the so-called α and β polypeptides, with a pigment to subunit stoichiometry of 2 and 3, respectively. It is still under discussion whether the LH1 complex completely encircles the RC in vivo. Other hypotheses are that in vivo the LH1

[†] This work was financially supported by The Netherlands Organization of Scientific Research (NWO) via the Foundation of Earth and Life Sciences (ALW) and by the NIH Grant GM R01-057175 for funding instrument development via a grant supplement.

* Corresponding author. Fax +31-20-4447999. Tel.: +31-20-4447166. E-mail: pandit@bio.vu.nl.

[‡] Department of Structural Biology, Vrije Universiteit Amsterdam.
[§] Departments of Chemistry and Physics, University of Illinois at Urbana-Champaign.

^{||} Faculty of Earth and Life Sciences and Division of Physics and Astronomy, Vrije Universiteit Amsterdam.

[⊥] Center for Biophysics and Computational Biology, University of Illinois at Urbana-Champaign.

¹ Abbreviations: BChl, bacteriochlorophyll; LH1, the core light-harvesting complex; LH2, the peripheral light-harvesting complex; RC, photosynthetic reaction center; OG, *n*-Octyl- β -D-glucopyranoside; CMC, critical micelle concentration; T-jump, temperature jump; fwhm, full width at half-maximum; DADS, decay-associated difference spectrum.

complex is shaped like a “horseshoe”, or that it consists of stacked dimers (7–9).

A remarkable property of the LH1 complexes of purple bacteria, such as *Rs. rubrum*, *Rps. marina*, *Rps. viridis*, and *Rb. sphaeroides*, is that they can be dissociated into their subunits by treatment with detergent and extraction of carotenoids (10–12). The subunits and the LH1 complex have been reconstituted from the separately isolated components (13, 14), and in one study the LH1 complex has been reconstituted together with isolated RCs, demonstrating that photosynthetic units can be reassembled in which excitation energy is successfully transferred to the RC (15). Interactions driving the assembly of subunits to form LH1 include the formation of hydrogen bonds between a subunit-pigment and Trp residues of the α -polypeptides of the preceding subunit and the formation of at least two ion pairs (16, 13, 17, 18). Presumably in vivo the α - and β -polypeptides are bound together and then inserted into the membrane before further oligomerization takes place (19), but the exact process of assembly in vivo is still unclear.

For *Rs. rubrum* a mutant strain, called G9, exists that produces LH1 antenna complexes lacking carotenoids. Isolated LH1 complexes of this strain, called B873 and absorbing at 873 nm, can be reversibly dissociated into subunits, called B820, absorbing at 820 nm, and further into monomeric pigment-ligated α - or β -polypeptides, called B777, absorbing at 777 nm (10, 20–23). For the B820–B777 dissociation reaction the stoichiometry and thermodynamics have been determined (11, 22–26). Depending on the detergent, polypeptide, and BChl concentrations, dimerization or tetramerization of the B777 monomers is possible (27). For the reassociation reaction of the LH1 complex from its subunits, intermediates have been observed (11, 22, 23, 28, 29), of which the most prominent one has an absorption maximum around 850 nm. Végh and Robert spectroscopically characterized this intermediate, which appears to be dimer of B820 subunits (30). In an earlier study we observed also other, less prominent, spectral intermediates that might reflect either small oligomers of B820 or large incomplete LH1 rings. Furthermore, our spectroscopic work on the LH1 association suggested a moderately cooperative assembly process for the B820–B873 reassociation. Recently a study appeared in which an oligomeric series of the LH1 complex of *Rb. sphaeroides* was isolated by gel electrophoresis and investigated spectroscopically (31). In agreement with our findings, their absorption and polarized fluorescence results could be explained by differently sized oligomers of heterodimers that form a curvilinear array of excitonically coupled chromophores.

In Figure 1 the absorption spectra are drawn of the LH1 complex (B873), its dimeric subunit form (B820), monomeric form (B777), and the supposed 850-nm absorbing intermediate (dotted line), of which the absorption spectrum has been resolved by global-analysis fitting of a set of absorption spectra in different stages of the B820–B873 reassociation reaction (23). Figure 1 illustrates that both dissociation of the LH1 complex into subunits and dissociation of the subunit into monomers are accompanied by a ~ 50 nm blue shift of the BChl absorption, due to a loss of excitonic coupling and hydrogen bonding between the pigments within the complex or within the subunit. Thereby the BChl pigments form intrinsic spectroscopic probes that sense the state of assembly,

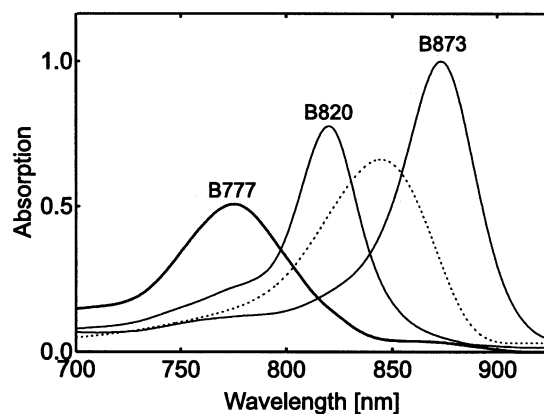


FIGURE 1: The absorption spectra of the LH1 complex (B873), its subunit form (B820) and monomeric form (B777) and the supposed spectrum of an intermediate structure (dotted line).

which in turn can be modulated by varying parameters such as detergent concentration, temperature, or protein concentration.

The currently known information about the structure and reconstitution of the LH1 complex, its subunits, intermediates, and possible assembly mechanisms makes it highly interesting to perform a kinetic experiment in which the (dis-)assembly of the complex or its subunits are followed. One of the few studies that attempted to follow these assembly kinetics were performed by van Mourik et al. (29). They investigated the spectral kinetics of the LH1 assembly reaction, by using a diode-array coupled stopped-flow apparatus. The reassociation kinetics could be fit assuming a two-step reaction, but structured residuals and a blue-shifted spectrum for the reassociated complex compared to native LH1 suggested that more intermediates might be present in the reaction. Other studies that investigated the in vitro assembly of membrane proteins included monitoring the folding of bacteriorhodopsin and the assembly of the light-harvesting chlorophyll *a/b* complex of photosystem II (LHCII) (32, 33). In all cases a stopped-flow apparatus was used and the assembly reaction was initiated by rapidly diluting out detergent or sodium dodecyl sulfate (SDS). A drawback of this technique is the limited time resolution of a stopped-flow apparatus and inherent mixing effects that have to be taken into account. We demonstrated in earlier studies that the full LH1 oligomerization reaction in vitro can not only be mediated by detergent, but also by changing the temperature over a range of 20 degrees (23). In addition to rapid mixing with detergent, a rapid temperature change could be applied to trigger the dissociation of the LH1 complex into subunits, or dissociation of the subunits into monomeric peptides. This provides us with a method for measuring the time-resolved kinetics without inherent mixing effects and on faster time scales, depending on the method used to create a temperature jump.

In this work we present a new approach to monitor the fast dissociation kinetics of a membrane protein. Using an infrared laser-induced temperature-jump setup, dissociation of the LH1 complex into its B820 subunits was induced. The time-resolved dissociation kinetics were followed as changes in the absorption at several wavelengths over a time window ranging from microseconds up to two hundred milliseconds. We demonstrate that this technique, which has been used for refolding studies of denatured water-soluble

proteins (34, 35), can be applied for study of membrane-protein disassembly kinetics.

1. MATERIALS AND METHODS

1.1. Sample. *n*-Octyl- β -D-glucopyranoside (OG) was obtained from Fisher Biotech (USA). Purified B820(OG) complexes were prepared from the carotenoidless strain *Rs. rubrum* G9 as described previously (23). Buffers were prepared in H₂O/D₂O mixtures instead of in H₂O, to reduce heat absorption of the sample upon a T-jump, so that a uniformly shaped heat pulse was created over the path lengths of the sample cell. Stock solutions of B820 subunits, solubilized in 0.8% OG, 50 mM K phosphate, pH 7.5, were diluted in H₂O/D₂O buffer to a final concentration of 76–80% D₂O, 50 mM K phosphate and 0.7% OG (preparing a sample equilibrated between B873 and B820) or 2% OG (preparing a sample equilibrated between B820 and B777). All measurements were carried out using a 1 mm quartz absorbance cell, placed in a thermo-electric temperature-controlled cuvette holder.

1.2. Temperature-Jump Induced Kinetics. Kinetics were initiated by a 10 ns near-infrared heating pulse. The 1.9 μ m heating pulse was produced by imaging the 1064 nm Nd:YAG laser beam into a Raman cell filled with H₂. It was split into two counterpropagating pulses to make the temperature profile more uniform in the interaction volume. Ninety percent of the heating pulse energy was absorbed by an OD overtone of D₂O. The average of temperature jump size was 5 °C with an inhomogeneity in the center axis less than 42%. Because of the small jump size, this inhomogeneity should not cause a significant spread of dissociation relaxation rates. Indeed, the rates observed for smaller 3 °C average T-jumps starting at the same temperature showed the same temperature trend and were only slightly slower, as expected for the 2 °C lower final temperature. The sample was thermostated with a recirculating bath and thermoelectric cooler, and read by a calibrated thermocouple. The temperature uncertainties resulting from inhomogeneity and calibration are shown in Table 1.

The dissociation reaction induced by the T-jump was monitored by transmittance changes at different wavelengths. We used a mode-locked Ti:Sapphire laser with a tuning range from 700 to 900 nm as the probe beam. Narrow-band 15 nm interference filters were placed in front of the sample cell to select the wavelengths. For the B877–B820 ring-dimer dissociation reaction, transmittance changes at 873, 850, and 820 nm were monitored: transmittance is expected to increase at the redder wavelength upon jumping to higher temperature when the equilibrium is shifted toward dissociation. For the B820–B777 dimer–monomer dissociation reaction, transmittance changes at 780 and 830 nm were monitored. Under conditions similar to the B873–B820 dissociation experiment, with respect to the sample preparation (protein and detergent concentration) and infrared apparatus (1.9 μ m heating pulse), a control experiment was performed in which the time-resolved transmittance was probed at 633 nm where there is no specific chromophore absorption. In this control experiment, no transmittance changes were observed after the first millisecond.

The T-jump induced dissociation reaction and the control measurement were detected by a 400 μ s rise time Si

Table 1: Results from Global-Analysis Fitting of δ Absorption Traces Probed at 820, 850, and 873 nm^a

T_i [°C]	T_f [°C]	τ [ms]	A_{820}	A_{850}	A_{873}
12(+/-0.5)	17(+1/-2)	2.5	0.4	0.3	0.7
		15	0.1	0.4	0.4
		120*	-0.4	0.6	0.7
		inf	0.8	-0.2	-0.7
14(+/-0.5)	19(+1/-2)	4.6	0.4	0.3	0.3
		67*	-0.4	0.5	0.7
		inf	0.8	-0.4	-0.7
16(+/-0.5)	21(+1/-2)	10	0.1	0.5	0.2
		68*	-0.5	0.3	0.6
		inf	0.8	-0.2	-0.8
20(+/-0.5)	25(+1/-2)	28*	-0.5	0.5	0.4
		120	-0.02	-0.02	0.3
		inf	0.8	-0.5	-0.7
25(+/-0.5)	30(+1/-2)	13*	-0.3	0.7	0.4
		33	0.3	0.3	0.3
		inf	0.2	-0.5	-0.6

^a T_i 's are the starting temperatures and T_f 's the final temperatures after application of the T-jump, with the uncertainties resulting from inhomogeneity and calibration errors between brackets. δ absorption traces were fit with two or three exponential-decay components and one nondecaying component, expressed by an infinite lifetime. Columns 3–6 present the fitted lifetimes and their associated amplitudes at 820, 850, and 873 nm respectively. The relative errors in the estimated parameters (lifetimes and amplitudes) are 5%. Lifetimes marked with an asterisk are assigned to inverse dissociation rates.

photodiode, and digitized by a LeCroy digital oscilloscope in 4 μ s/pt sampling rate. Data were collected from -20 ms to 180 ms with respect to the T-jump pulse.

1.3. Global Fitting. Data were fitted using a global-analysis fitting procedure. For data analysis, transmittance traces were converted into delta absorption traces, and for each thermostated temperature, data probed at 873, 850, and 820 nm were fitted simultaneously. Next to a stepfunction (infinite lifetime), two or three exponential decays were needed for adequate fitting. Plots of the amplitudes associated with the lifetimes vs the three probe wavelengths represent very rough delta-absorption difference spectra (DADS) that can give some insight into the actual spectroscopic processes to which the kinetics are related (36).

2. RESULTS AND DISCUSSION

2.1. Dissociation of B820 Subunits into B777 Monomers. The kinetics of the B820–B777 dissociation reaction were monitored as transmittance changes at 780 and 830 nm, upon applying a T-jump on a sample prepared in 2% OG. The sample was thermostated at 15, 20, 25, and 29 °C, to perform T-jumps at different stages of the B777–B820 equilibrium.

Figure 2 shows an example of delta absorbance traces probed at 830 and 780 nm for a sample thermostated at 15 °C. At time zero T-jumps are applied, resulting in a fast decrease of absorbance at 830 nm and rise of absorbance at 780 nm, as B820 subunits are dissociated into B777 monomers. The absorbance changes occur in about 500 ms. This lifetime is the rise time of the diode, and we conclude that the major part of the dissociation equilibrium takes place within this response time. The slow recovery phase could be caused by slow temperature relaxation. Absolute absorbance changes probed at 780 nm are smaller than the ones probed at 830 nm, in agreement with the relatively low

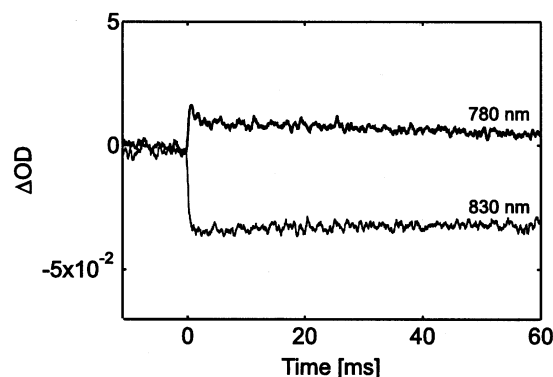


FIGURE 2: Delta absorption traces probed at 830 nm (near the maximum of the B820 subunit) and at 780 nm (near the maximum of the B777 monomer). At time zero, a T-jump is applied starting at 15 °C. The sample contained 5 times diluted stock solution of purified B820 (stock $OD_{820} = 28 \text{ cm}^{-1}$) solubilized in 2% OG.

extinction coefficient of B777 at 780 nm compared to the extinction coefficient of B820 at 830 nm (see Figure 1).

Fast dissociation kinetics are to be expected. The dissociation reaction should not include the breaking or formation of detergent micelles because the sample was prepared in OG at a concentration high above the critical micelle concentration (CMC) of OG. The dissociation kinetics probably involves the kinetics for breaking of two hydrogen bonds, as it is proposed that in the B820 subunit the BChl pigment bound to the α -polypeptide is hydrogen-bonded to the His residue of the β -polypeptide and vice versa (37, 4).

2.2. Dissociation of B873 into B820 Subunits. The kinetics of B873–B820 equilibration were monitored by time-resolved transmittance at 820, 850, and 873 nm, after applying a T-jump to samples prepared in 0.7% OG. The probe wavelengths at 820 and 873 nm were chosen at the maximum absorption of B820 (dimer) and B873 (ring). The probe wavelength at 850 nm was chosen because in steady-state measurements intermediate structures with an absorption maximum around 850 nm had been observed (23). The sample was thermostated at temperatures between 12 and 25 °C (Table 1), to start T-jumps at different B873–B820 equilibria.

The upper panels of Figure 3 show δ absorption traces of a sample thermostated at 12 (A) and 20 °C (B), together with the fit curves. The lower panels show low-resolution DADS associated with the lifetimes of the fitting curves. The 120 ms DADS in C and the 28 ms DADS in D (triangles) show that absorption disappears at 873 and 850 nm and appears at 820 nm. The nondecaying components (circles in Figure 3C,D) have the opposite amplitude trend, and these DADS represent the difference spectra of equilibration at the initial temperature and at the final temperature after the T-jump. δ absorption traces of the sample T-jumped at other temperatures (not shown) also yielded a lifetime component associated with spectral changes in which absorption at 873 and 850 nm disappears and absorption at 820 nm appears. Their nondecaying components again show the opposite trend. Hence, those lifetimes represent the kinetics by which B873–B820 equilibrium is reached, with a larger final B820 population. These lifetimes decreased from 120 (12 °C) to 13 ms (25 °C, see Table 1). Around 20 °C, the sample was roughly equilibrated evenly between B820 and B873. By using the equilibrium constant $K_{eq} \approx 1$

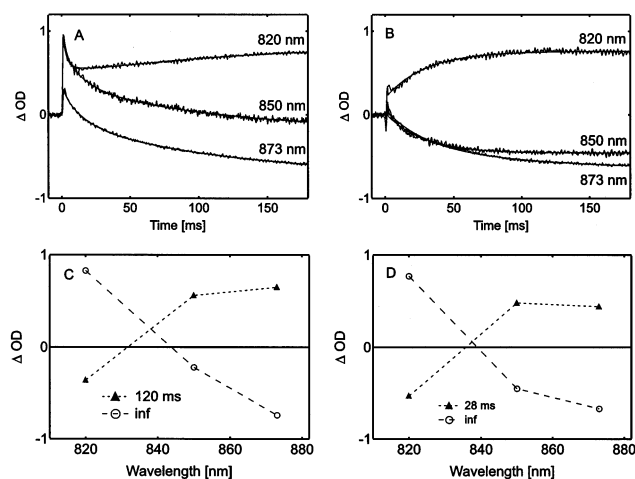


FIGURE 3: Upper panel: delta absorption traces probed at 820 nm (absorption max. of the B820 subunit), at 850 nm (absorption max. of intermediate structures), and at 873 nm (absorption max. of the B873 complex), together with the multiexponential fit functions. At time zero a T-jump is applied at 12 (A) and 20 °C (B). The absorption levels at time zero were 0.2 (820 nm), 0.07 (850 nm), and 0.37 (873 nm) at 12 °C and 0.38 (820 nm), 0.25 (850 nm), and 0.29 (873 nm) at 20 °C. Lower panel: the estimated amplitudes at the three probe wavelengths associated with the B820–B873 dissociation lifetimes resulting from multiexponential fitting of delta absorption traces at 12 (C) and 20 °C (D). The sample contained 6.5 times diluted stock solution of purified B820 (stock $OD_{820} = 38 \text{ cm}^{-1}$) solubilized in 0.7% OG.

at 20 °C for the B873–B820 reaction and simplifying the treatment of the interconversion to two-state (dissociation of B873 directly into B820 subunits), we obtain $k_{\text{association}} \approx k_{\text{dissociation}} \approx 18 \text{ s}^{-1}$ at 20 °C.

In the stopped-flow experiment by van Mourik et al. (29) a rate of about 10 s^{-1} was observed for association of B820 subunits toward a B873-like complex. They started the reaction from an equilibrium in which only B820 subunits were present, rapidly diluting the detergent concentration to induce association. We note here that their observed rate (presumably reflecting the association rate) is on the same order as the association rate we found here. This enhances the idea that both experiments describe the same reaction process, although in their study the reaction was triggered by changing the detergent concentration, whereas in this experiment it was triggered by a fast temperature change.

In addition to the B873–B820 equilibration, several other kinetic components show up in the data. Table 1 gives an overview of the fitted lifetimes and amplitudes at the three probe wavelengths, obtained from data collected for T-jumps at different thermostated temperatures. Traces for T-jumps at 12 °C were fit with four components (upper four rows), and traces for T-jumps at the other four temperatures were fit with three components. Each row presents the lifetime and its associated amplitudes at 820, 850, and 873 nm of one fit component. The lifetimes corresponding to the kinetic components attributed to B873–B820 dissociation kinetics are marked with an asterisk. The nondecaying components are presented as the amplitudes associated with the “infinite” lifetimes.

Table 1 shows a set of fast lifetimes in the 2.5 to 33 millisecond range, with positive amplitudes at all three probe wavelengths (decrease of absorption). These are less easy to interpret. In stopped-flow experiments performed by

others, lifetime components on the order of 10 ms were attributed to the process of micelle-mixing (32, 33). Though no mixing takes place in our experiments, the dissociation reaction probably involves formation of protein/detergent micelles if the B873–B820 dissociation reaction is coupled with a phase transition of the detergent from below to above the CMC (23). Lifetimes that have similar amplitudes for all three probe wavelengths (probe wavelength independent process) could include the effects of micellization. As noted in the Materials and Methods section, in a control experiment no transmittance changes were observed after the first millisecond, and a change in absorption on longer time scales therefore cannot simply be assigned to scattering. Possibly, the dissociation reaction is preceded by local structural changes (such as a rearrangement of detergent molecules surrounding the complexes) that change the pigment absorption properties.

The absorption level probed at 850 nm, at time zero before T-jumps were applied, was raised after some jump-experiments. This suggests that intermediate structures are formed. In an earlier study, no intermediates were observed in steady-state absorption spectra of LH1 samples, in which the temperature was raised incrementally, but they occurred in recooled samples (23). Intermediates might have accumulated here in the course of the experiment if dissociated complexes reassociated after temperature relaxation and got trapped in intermediate states. In addition to the bulk dissociation reaction of B873, side reactions might have occurred in which intermediates were dissociated into B820 subunits. It should be reminded here, that the interference filters used for probe wavelength selection have a width of 15 nm fwhm and allow that some B873 absorption is probed at 850 nm and that absorption of intermediate structures is probed at 873 nm and at 820 nm. Because of such experimental limitations, we here cannot distinguish detailed spectral changes here and therefore focus on the bulk dissociation reaction of the LH1 (B873) complex. Future experiments will have to gauge the involvement of intermediates in the dissociation process.

We did not observe that the dissociation reaction of B873 into B820 subunits appeared via intermediate states. However, intermediates might be formed within a time scale of a few milliseconds and its appearance obscured by other kinetics on this time scale, of which the origin is not clear at this point.

3. CONCLUSION

We determined the dissociation rate by which isolated LH1 complexes (B873) solubilized in 0.7% OG (onset of the CMC) are dissociated into dimeric subunits:



This reaction occurred on time scales varying from 120 ms at 12 °C down to 13 ms at 25 °C, with a two-state rate of $k_{\text{association}} = 18 \text{ s}^{-1}$ when $K_{\text{eq}} \approx 1$.

Furthermore we investigated the time-resolved dimeric dissociation of B820 subunits into B777 monomers, solubilized in 2% OG (well above the CMC):



This reaction appeared to occur within 500 μs , which was

the response time of our detection system. The kinetics of reaction scheme 1 are probably influenced by the rate of protein-detergent equilibration, as the protein was solubilized with detergent under conditions near the CMC. In fact, dissociation of the B873 ring complex into B820 subunits and of its B820 subunit into B777 monomers should include similar processes such as breaking of hydrogen bonds and ion pairs and the formation of both is driven by efficient packing of the polypeptides and hydrophobic interactions. Therefore, it would be relevant to resolve the true kinetics for dissociation of B820 into B777 monomers, as this process can be accomplished under high detergent concentrations where no detergent phase transition takes place.

The experiment has demonstrated that an infrared laser-pulsed temperature jump can be applied to trigger dissociation of the LH1 complex in vitro and that this technique has potential for studying the disassembly reaction dynamics and thermodynamics of this complex. More elaborate experiments, for instance, under different detergent conditions and probing at different wavelengths simultaneously, should be conducted to resolve details of the B873–B820 dissociation reaction. It would be highly interesting to determine the level of cooperativity for dissociation of the LH1 ring into B820 subunits, which might proceed via intermediate states absorbing at 850 nm and as a gradual process via the occurrence of uncompleted rings and formation of small aggregates.

REFERENCES

1. van Grondelle, R., Dekker, J. P., Gillbrö, T., and Sundström, V. (1994) *Biochim. Biophys. Acta* 1187, 1–65.
2. Sundström, V., Pullerits, T., and van Grondelle, R. (1999) *J. Phys. Chem. B* 103, 2327–2346.
3. McDermott, G., Prince, S. M., Freer, A. A., Hawthornthwaite-Lawless, A. M., Papiz, M. Z., Cogdell, R. J., and Isaacs, N. W. (1995) *Nature* 374, 517–521.
4. Koepke, J., Hu, X., C.Muenke, Schulten, K., and Michel, H. (1996) *Structure* 4, 581–597.
5. Karrasch, S., Bullough, P. A., and Ghosh, R. (1995) *EMBO J.* 14, 631–638.
6. Hu, X., and Schulten, K. (1998) *Biophys. J.* 75, 683–694.
7. Frese, R. N., Olsen, J. D., Branvall, R., Westerhuis, W. H. J., Hunter, C. N., and van Grondelle, R. (2000) *Proc. Natl. Acad. Sci. U.S.A.* 97, 5197–5202.
8. Jungas, C., Ranck, J.-L., Rigaud, J.-L., Joliot, P., and Verméglio, A. (1999) *EMBO J.* 18, 534–542.
9. Francia, F., Wang, J., Venturoli, G., Melandri, B. A., Barz, W. P., and Oesterhelt, D. (1999) *Biochemistry* 38, 6834–6845.
10. Miller, J. F., Hinchigeri, S. B., Parkes-Loach, P. S., Callahan, P. M., Sprinkle, J. R., Riccobono, J. R., and Loach, P. A. (1987) *Biochemistry* 26, 5055–5062.
11. Visschers, R. W., and van Grondelle, R. (1992) *Biochim. Biophys. Acta* 1100, 259–266.
12. Meckenstock, R. U., Krusche, K., Brunisholz, R. A., and Zuber, H. (1992) *FEBS Lett.* 311, 128–134.
13. Davis, Ch. M., Parkes-Loach, P. S., Cook, Ch. K., Meadow, K. A., Bandilla, M., Scheer, H., and Loach, P. A. (1996) *Biochemistry* 35, 3072–3084.
14. Parkes-Loach, P. S., Sprinkle, H. J. R., and Loach, P. A. (1988) *Biochemistry* 27, 2718–2727.
15. Bustamante, P. L., and Loach, P. A. (1994) *Biochemistry* 33, 13329–13339.
16. Davis, Ch. M., Bustamante, P. L., Todd, J. B., Parkes-Loach, P. S., McGlynn, P., Olsen, J. D., McMaster, L., Hunter, C. N., and Loach, P. A. (1997) *Biochemistry* 36, 3672–3679.
17. Parkes-Loach, P. S., Michalski, T. J., Bass, W. J., Smith, U., and Loach, P. A. (1989) *Biochemistry* 29, 2951–2960.
18. Sturgis, J. N., Olsen, J. D., Robert, B., and Hunter, C. N. (1997) *Biochemistry* 36, 2772–2778.
19. Drews, G. (1996) *Arch. Microbiol.* 166, 151–159.

20. Ghosh, R., Hauser, H., and Bachofen, R. (1988) *Biochemistry* 27, 1004–1014.
21. Chang, M. C., Callahan, P. M., Parkes-Loach, P. S., Cotton, Th. M., and Loach, P. A. (1990) *Biochemistry* 29, 421–429.
22. Loach, P. A., and Parkes-Loach, P. S. (1995) in *Anoxygenic Photosynthetic Bacteria* (Blankenship, R. E., Madigan, M. T., and Bauer, C. D., Eds.) Chapter 21, pp 437–471. Kluwer Academic Publishers, Dordrecht, The Netherlands.
23. Pandit, A., Visschers, R. W., van Stokkum, I. H. M., Kraayenhof, R., and van Grondelle, R. (2001) *Biochemistry* 40, 12913–12924.
24. Sturgis, J., and Robert, B. (1994) *J. Mol. Biol.* 238, 445–454.
25. Meadows, K. A., Parkes-Loach, P. A., Kehoe, J. W., and Loach, P. A. (1998) *Biochemistry* 37, 3411–3417.
26. Kehoe, J. W., Meadows, K. A., Parkes-Loach, P. A., and Loach, P. A. (1998) *Biochemistry* 37, 3418–3428.
27. Arluison, V., Seguin, J., and Robert, B. (2002) *FEBS Lett.* 516, 40–42.
28. Beekman, L. M. P., Steffen, M., van Stokkum, I. H. M., Olsen, J. D., Hunter, C. N., Boxer, S. G., and van Grondelle, R. (1997) *J. Phys. Chem. B* 101, 7284–7292.
29. van Mourik, F., Corten, E. P. M., van Stokkum, I. H. M., Visschers, R. W., Loach, P. A., Kraayenhof, R., and van Grondelle, R. (1992) in *Research in Photosynthesis* (Murata, N., Ed.) pp 101–104. Kluwer Academic Publishers, The Netherlands.
30. Végh, A. P., and Robert, B. (2002) *FEBS Lett.* 528, 222–226.
31. Westerhuis, W. H. J., Sturgis, J., Ratcliffe, E. C., Hunter, C. N., and Niederman, R. A. (2002) *Biochemistry* 41, 8698–8707.
32. Booth, P. J., and Paulsen, H. (1996) *Biochemistry* 35, 5103–5108.
33. Booth, P. J., and Farooq, A. (1997) *Eur. J. Biochem.* 246, 674–680.
34. Ballew, R. M., Sabelko, J., Reiner, C., and Gruebele, M. (1996) *Rev. Sci. Instrum.* 67 67, 3694–3699.
35. Sabelko, J., Ervin, J., and Gruebele, M. (1999) *Proc. Natl. Acad. Sci. U.S.A.* 96, 6031–6036.
36. Holzwarth, A. R. (1996) in *Techniques in Photosynthesis* (Amesz, J., and Hoff, A. J., Eds.) pp 75–92. Kluwer Academic Publishers, The Netherlands.
37. Olsen, J. D., Sturgis, J. N., Westerhuis, W. H. J., Fowler, G. J. S., Hunter, C. N., and Robert, B. (1997) *Biochemistry* 36, 12625–12632.

BI0269005